Sci. Technol. Arts Res. J., Jan. – March 2024, 13(1), 67-82
DOI: https://doi.org/10.20372/star.v13i1.05
ISSN: 2226-7522 (Print) and 2305-3372 (Online)
Science, Technology and Arts Research Journal
Sci. Technol. Arts Res. J., Jan. – March 2024, 13(1), 67-82
Journal Homepage: https://journals.wgu.edu.et

Original Research

Anti-oxidant studies on phyto mediated synthesis and characterization of ZnO Nanoparticles using *Croton macrostachyus* Leaf Extract

Tola Jabessa Masho[1,2*], Ponnusamy Thillai Arasu[1], Raji Feyisa Bogale[1], & Addisalem Abebe[3]

[1]Department of Chemistry, College of Natural and computational Sciences, Wollega University, Nekemte, Post Box No. 395, Ethiopia
[2]Department Chemistry, College of Natural and computational Sciences, Blue Hora University, Post Box No 144, Bule Hora, Ethiopia
[3]Department of Chemistry, College of Natural and Computational Sciences, Arba Minch University, Arba Minch, P.O. Box 21, Ethiopia

Abstract

The size range of nanomaterials spans from one nanometer to one hundred nanometers. Nanomaterials synthesized from metal oxides using phytochemical extracts from plants are currently quite popular owing to their wide range of potential uses. The researcher in this study so concentrated on producing ZnO nanoparticles by solution-burning a water-based extract from the Croton macrostachyus plant. Flavonoids, tannins, and phenolic compounds are some of the secondary metabolites of Croton macrostachyus that may help with the phyto-mediated synthesis of nanoparticles by reducing their size, stabilizing them, and sealing them. In order to create ZnO nanoparticles, this research utilized the precursor Zn $(CH_3COO)_2.3H_2O$. The synthesized samples were characterized using a variety of imaging techniques, including powder X-ray diffraction, Fourier transform infrared, ultraviolet, visible, and diffuse reflectance, X-ray photoelectron, imaging electron microscopy, scanning electron microscopy with energy dispersive X-ray, and a high-resolution imaging electron microscope. Although DDPH and ZnO nanoparticles exhibited lower scavenging activity than ascorbic acid at low concentrations, this improved with increasing sample concentration. The optical band gap energy of ZnO nanoparticles was 3.20 eV.

Article Information

Article History:
Received: 12-01-2024
Revised : 20-02-2024
Accepted : 30-03-2024

Keywords:
XPS, SEM-EDX, HRTEM, Phyto- mediated and anti-oxidant activities

*Corresponding Author:
Tola Jabessa Masho

E-mail:
tolajabessa2019@gmail.com

INTRODUCTION

The main goal of nanotechnology is to make it easier to produce nanomaterials with exceptional utilization proficiency and distinctive properties by employing green synthesis techniques. (Tanna et al., 2016). Nanomaterials with sizes between 1nm to 100 nm in length are known as nanoparticles. Because of their distinct benefits over bulk materials owing to their smaller size, metal oxide nanoparticles and nanocomposites have

found substantial uses in a range of industries recently (Ahmed et al., 2017). Notably, this involves sensors in a variety of industries, such as textiles, agriculture, medicine, pharmacy, and catalysis. (Peralta-Videa *et al*., 2016 and Mutukwa et al., 2022). The chemical synthesis of metal oxide nanoparticles or composites was found to be unsuitable due to toxic byproducts, high costs, and a lack of environmental friendliness. In contrast, phyto-mediated synthesis employed secondary metabolites functioning as reducing, stabilizing, and capping agents in the plant extract. As a result, environmentally friendly and green nanoparticle synthesis methods were developed to address these issues. As stated before by different researchers green synthesis, using plant extracts such as *Euphorbia abyssinica* plant bark extract (Faye et al., 2022), and *Parthenium hysterophorus* (Najoom et al., 2021), by the solution combustion method. Therefore based on this reports the green method synthesis was more significant than the others. Though the process different investigation reports were indicating that more phytochemicals, which are used as stabilizing and reducing agents were present in the traditional medicinal plant extract (Danish et al., 2020 and Chen et al., 2020), certain examples of methods were, among alternative approaches consist of the employing of ball mills, sol-gel synthesis, micro emulsions, and liquid-state microbiological procedures. Due to the significant amount of secondary metabolites including flavonoids, tannins, and alkaloids the plant *Croton macrostachyus* is widely available in Ethiopia and other neighboring nations. It is used in traditional medicine deployed cure for a variety of illnesses especially diarrhea, fungal infections, wounds, malaria, and diabetic until later (Maroyi et al., 2017) So some modification of solution composition methods was used and ant oxidant activity was investigated (Mansoori et al., 2020).Therefore in this current work, The researcher used the *Croton macrostachyus* leaf extract was used for synthesis of ZnO nanoparticles

MATERIALS AND METHODS

Instruments and Apparatus

In the present study, glass rod, quartz cuvettes , hotplate with magnet stirrer, crucibles, 40, 75, 100, 500 and 1000 mL beakers, a mechanical grinder, pH meter, what man filter paper No.1, there were also graduated glassware with different sizes and Erlenmeyer flask with varies shapes and sizes. Powder X-ray diffraction (PXRD), Fourier transforms infrared spectra (FTIR), UV-visible diffuse reflection spectroscopy, UV-visible spectroscopy (UV-Vis) and X-ray photoelectron spectroscopy (XPS), the instruments used for the sample analysis were Selected Area Electron Diffraction Analysis (SAED), High-Resolution Transmission Electron Microscope (HRTEM), Transmission Electron Microscopy (TEM), Energy Dispersive X-ray (EDX) and Scanning Electron Microscopy (SEM)

Reagents and chemicals

The substances(chemicals) and reagents employed were zinc acetate dihydrate caustic soda (98% NaOH), aqueous solution of hydrogen chloride (HCl, 18%), ethanol (CH_3CH_2OH 99.9%), potassium hydroxide(KOH, 99%), iodine (I_2, 99%),

dimethyl sulfoxide (DMSO, 99.5%), DPPH 2, 2-diphenyl-1-picrylhydrazyl, ascorbic acid ($C_6H_8O_6$), iron chloride ($FeCl_2$, 97%), sulphuric acid (H_2SO_4, 98%), DI water, and 100% methanol (CH_3OH) and a leaf extract of *Croton macrostachyus*, a plant, were used in the present study.

Plant sample extractions

In February 2023, fresh leaves of the *Euphorbiaceous* species called *Croton macrostachyus Hochst.* Ex Delile, were collected from the Botanical Garden Department of Biology at Wollega University, Nekemte, Ethiopia. Other colloquial names for the plant are *Makkaanisa* (Afan Oromo) and *Bisana* (Amharic). The leaves were routinely cleaned with tap water, then dried in the shade for three days to eliminate any residual moisture, and then checked with deionized water to remove any remaining dust. Using a mechanical mixer, dry samples were crushed and then powdered using a mortal and pistil. In 300 mL conical flasks with 200mL of methanol 30 g of the *Croton macrostachyus* leaf powder plant material was used in the extractions after that, the flasks were enclosed with aluminum foil.

Phytochemical Screening

Based on the color responses using established techniques, initial phytochemical screening of the leaf extracts from *Croton macrostachyus* in methanol was finalized (Masho *et al*., 2024).

Table 1

Croton macrostachyus leaf extract phytochemical test

Compound ingredients	Approaches	References
Alkaloids	Mayer's reagent	(Ram & Sinha, 2015)
Carbohydrates	Molisch test	(Parbuntari *et al*., 2018)
Flavonoid	Croton macrostachyus leaf extract was subjected to Alkaline test and diluted sodium hydroxide Before diluted H_2SO_4 was added.	(Dey *et al*., 2020)
Phenol	Ferric chloride test (two milliliters of diluted H_2SO_4 Solution was put to 5 milliliters of Croton macrostachyus DI water extract).	(Singh et al., 2017)
Tannins	Ferric chloride test (0.5 gram of croton leaf extracts mixed with 10 milliliters of bromine water)	(Saptarini et al., 2016)
Saponins	Foaming test using an alkaline reagent (5.0 ml of DI combined with a few drops of olive oil)	(Gul et al., 2017)

Zinc oxide (ZnO) nanoparticle synthesis

In order to create ZnO nanoparticles, 40 mL of *Croton macrostachyus* leaf extract and 50 mL of methanol were added in a 100 mL beaker along with zinc acetate dihydrate and the liquid was vigorously agitated for 50 minutes at 45^0C using a magnetic stirrer. This process produced high yield of zinc oxide nanoparticles by adding 2M NaOH to maintain the pH to 10. Subsequently, the white solution turned into a ZnO NPs as precipitate. This was quickly cleaned of contaminants using before being dried in an oven at 105°C, ethanol and deionized water are added. In order to achieve excellent XRD data and high crystallinity, the sample was calcined at 500°C for two hours in a furnace. Ultimately, the white powder was kept in storage to be further studied

Characterizations ZnO Nanoparticles

Double-beam UV-Vis spectrophotometer (Shanghai Drywell Scientific Instrument) was used to measure the absorbance & wavelength (200-800 nm) of ZnO nanoparticles. The band gap was found using UV-visible spectroscopy and UV-visible diffuse reflectance spectroscopy. A FTIR spectrum in the 4000-400 cm^{-1} range has been used to ascertain whether synthesized materials having any residual functional groups were present following calcination. The nature of the crystallinity was confirmed by PXRD (Shimadzu Corporation (Japan); PXRD7000), and size was determined using Scherer equations and unit cell parameters. SEM, EDX, TGA, TEM, HRTEM and XPS were used for size, morphology and elemental composition of synthesized ZnO NP's samples.

Anti-oxidant activities

Using a DPPH (2, 2-diphenyl-1-picrylhydrazyl) radical scavenging experiment, a serial dilution of two-fold (100, 50, 25, 12.5, 6.25, and 3.125 µg/ml) was made to investigate the antioxidant activity. The stock solution used was 1 mg/mL, and methanol was used as the solvent with slight modifications, the antioxidant activity of the synthesized ZnO NPs and ascorbic acid as a solvent was examined as previously reported (Elemike et al., 2020). In summary, 30µL of phyto mediated zinc oxide nanoparticles at various concentrations (2.00 µg/ml to 100 µg/ml) in 100% CH_3OH were treated with 100µL of DDPH. After 30 minutes in a dark, room-temperature surroundings, the color changed, and each sample's absorption at 517 nm was measured in different concentrations. The testing procedure employed the acid ascorbic as the standard (Elemike et al., 2020; and Chong et al., 2018).

$$\text{Radical Scavenging (\%)} = \left(\frac{Ab_{control} - Ab_{sample}}{Ab_{control}}\right) \times 100\% \quad (1)$$

Where Ab_{sample} is the absorbance of the DDPH solution with sample absorbance, and $Ab_{control}$ is the absorbance of the DDPH solution in ascorbic acid.

Data Analysis

The data related to XRD was drawn by using origin version 8, software released in year 2022.

RESULTS AND DISCUSSION

Screening potential phytochemicals

The secondary metabolites' alkaloids, flavonoids, phenols, tannins, carbohydrates and the saponins were found in the plant leaf extract by methanol solvent, in accordance with the results of phytochemical screening. This result is consistent with the prior *Croton macrostachyus* leaf phytochemical screening results (Terefe et al., 2022). These secondary metabolites' ability to exist allows them to be employed as reducing and stabilization agents when ZnO nanoparticles are being synthesized. The chemical components of the *Croton macrostachyus* leaf are presented in Table 2, which also displays the reagent used and the color change that was seen. This has been used as fuel in the synthesizing process of ZnO NPs (Cahino et al., 2019; Masho et al., 2024).

Table 2

Outcomes of a phytochemical screened leaf plant extract of the species Croton macrostachyus

Chemical component	Methods	Reflection	Results
Alkaloids	Test of Mayer's Reagent	Reddish brown precipitate / Precipitation of a greenish-colored cream precipitate.	+
Flavonoids	Test for Alkali used	A bright yellow changed to colorless	+
Carbohydrates	Molisch test	Growth of the violet ring at the joint	+
Phenol	Ferric chloride test	Growth of a dark green	++
Tannins	Ferric chloride	De coloration of bromine water	+
Saponins	Olive oil test	Presence of foam	+

Footnote; the "+" and "++" indicates; the presence of phytochemicals in C.macrostachyus more and most respectively

Characterization of phyto-mediated synthesized ZnO NPs,

UV-visible spectroscopy of ZnO NPs,

It was observed in (Figure 1, A & B), the surface plasmon resonance with the strongest absorption shows at maximum wavelength was 265 nm for *Croton macrostachyus* plant leaf extract and 363 nm for synthesized ZnO NP's is comparable with the earlier findings of ZnO nanoparticles was evident that the color of the reaction media changed from dark brown to colloidal light brown. As soon as the ground state nonbonding electrons are released, this is the surface plasmon resonance (SPR) indicator (Figure 1 C). The band gap energy is estimated by the formula:

$$\lambda g = 1239.8 / Eg \quad (2)$$

Where λg is band gap wavelength and Eg is the band gap energy. Therefore, decreases in band gap energy enhance the anti-oxidant activities (Ahmad et al., 2020 and Masho *et al*., 2024).

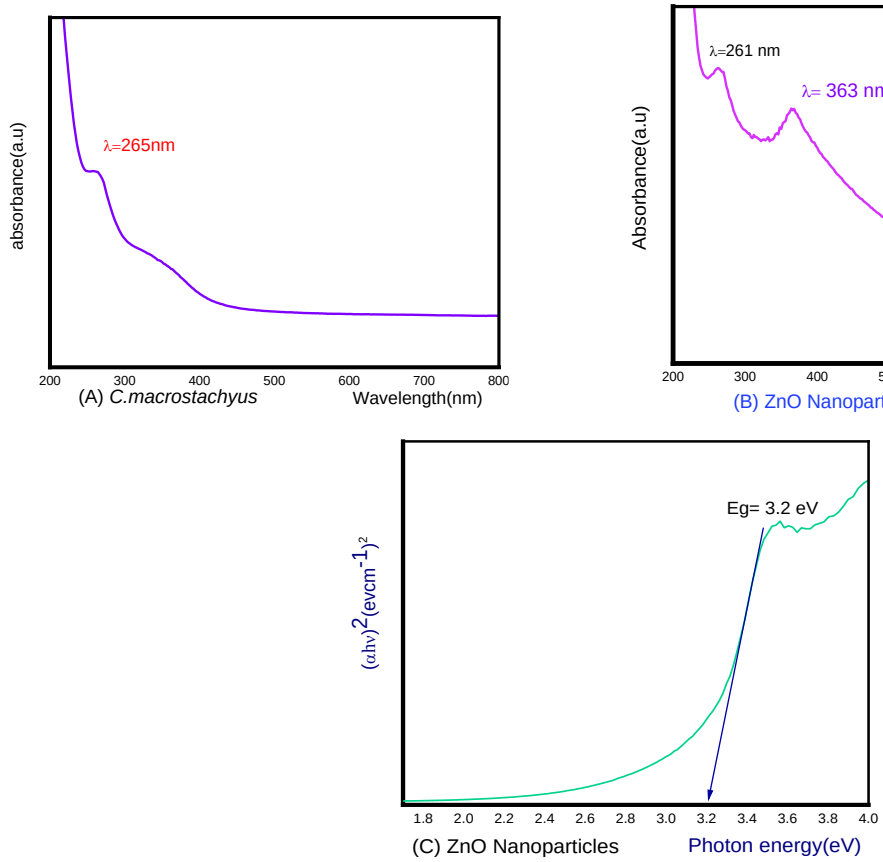

Figure 1.*UV-visible spectrum of Croton macrostachyus Leaf extracts (A), ZnO NPs (B) and Tauc's plot revealing the (C) ZnO NPs' optical band gap energy.*

UV-visible spectroscopy of diffuse reflectance

The lowering of band gap energy of ZnO NPs was determined by UV-visible diffuse reflectance spectroscopy with Tauc's plot (Figure 2 A & B). This is mainly due to the combined transition this decrease in the band gap energy was observed (3.24 eV) from Tauc's plot of UV-visible spectroscopy and UV-Vis DRS, as revealed.

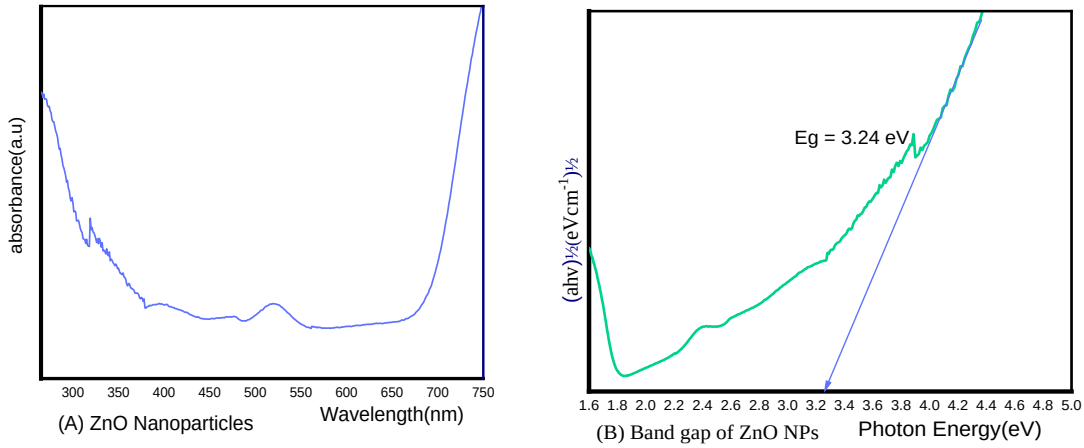

Figure 2. *Diffuse Reflectance in UV-Vis Spectroscopy band gap energy spectra (A, B)*

Thermal analysis (TGA /DSC)

TGA curves of the biosynthesized sample heated to 10^{o}C/min. The TGA profile shows a continual decrease in weight as shown in the Figure 3, the TGA/DSC examination was conducted. It is used to determining weight loss percentage and heat stability of the ZnO NPs sample. The probed nanoparticles weight loss was examined and it was found that the temperature range between 25°C and 100°C caused the greatest weight mass loss. This is because the water that was absorbed by the sample began to evaporate. As the temperature rise from 300°C to 550°C, the weight loss persisted. This could be because complexes generated from plant leaf extracts and the breakdown of $Zn(OH)_2$ was removed, and crystalline was created, as there was no weight loss between 550°C and 900°C. According to the plot shown, the sample (10 mg) completely lost weight between 25°C and 900°C.

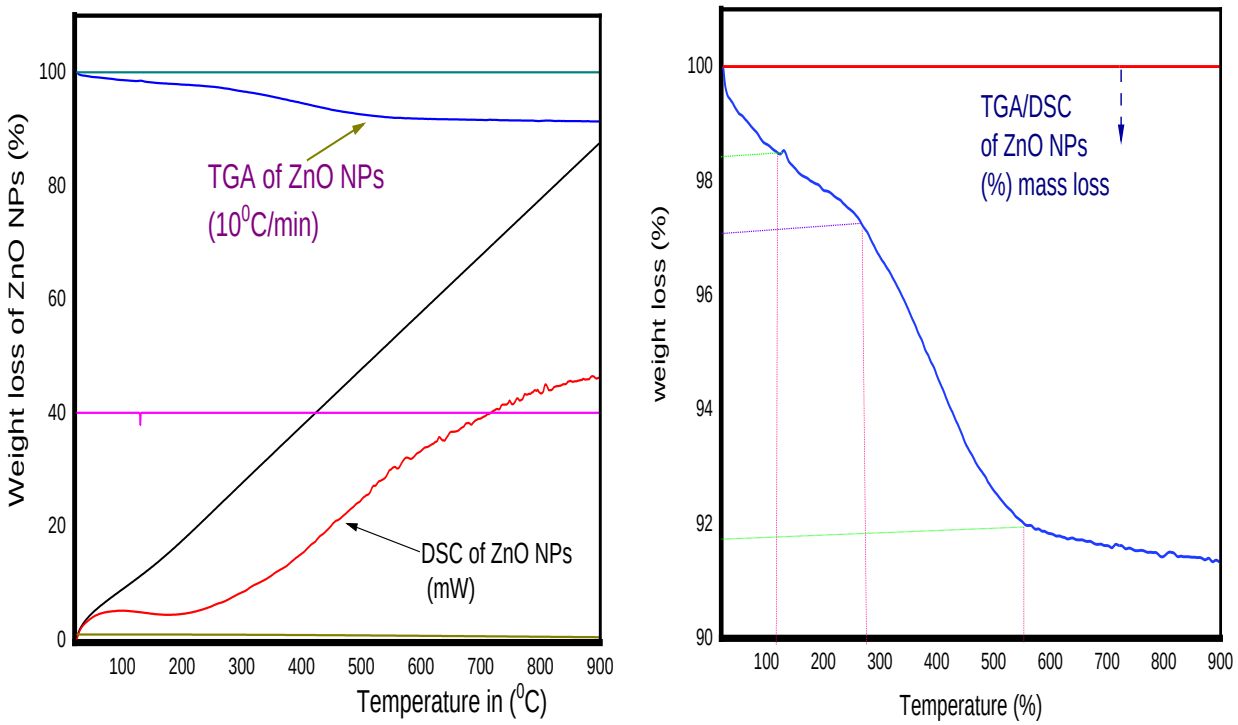

Figure 3. *Thermal analysis (TGA & DSC)*

FTIR spectra analysis

Using FTIR spectrophotometer, the functional groups of the metal oxide nanoparticles synthesized by phyto-mediated methods were examined in the range of 400cm^{-1} to 4000 cm^{-1}. The investigation's results are shown in Figure 4 (A & B), using FTIR validations. The samples of *Croton macrostachyus* leaf extract (3241.89, 2930.38 & 2343.01 cm$^{-1)}$, ZnO nanoparticles showed peak at 3241.89 cm^{-1}. These were comparable functional groups based on earlier reports (Terefe, et.al. 2022) of OH functional groups found at frequencies between 3700 and 3000 cm^{-1}. The ZnO NPs peak obtained at 863.28 cm^{-1} could have been produced by vibrations in the bonds between zinc and oxygen. At various wavelengths,

other functional groups were identified, including aromatic hydrocarbons, C=O, and C-H groups. As seen in Table 3, and Functional groups detected in *Croton macrostachyus* leaf extract were used in the reaction processes as stabilizing and capping agents in the synthesis of ZnO nanoparticles, the different vibration of bonds like Zn-O as it was reported the *Croton macrostachyus* leaf extracts constituents (Masho *et al*., 2024).

Table 3

FTIR for Croton macrostachyus leaf extract, ZnO NPs,

Absorption bands of *Croton macrostachyus* extract (cm^{-1})	Absorption bands ZnO NPs(cm^{-1})	explanation of the bending, vibrating, and stretching bonds
3241.89 2930.38 2343.01	3253.78	O-H stretch, free hydroxyl alcohols, phenols 3500–3200 (in alcohol, 3640–3610 Phenols, H-bonded alcohols, and O-H stretch 3400–3250 (m) (Terefe, et.al., 2022)
1624.01 1557.58	1559.28	N–H bend amines, 1650–1580 and C–C stretch (in–ring) aromatics, 1600–1585 carboxylate ions' carbonyl groups that are able to stay adsorbed on ZnO and CuO surfaces (Qin et al.,2017)
1402.51 1306.64	1402.96	1470–1450, bend alkanes C–H 1370–1350 C–H alkanes in rock
995.48	1049.58 1019.61 924.80 863.28	1250–1020, Alkyl-N stretch amines 910–665 N–H wag amines 900–675 C-H aromatic compounds The peak is assigned to Zn–O stretching and vibration frequency
661.87	775.89 650.90	oscillation/extension Zinc Oxide Zn-O NPs' stretching vibration, Given that absorption at this wavelength was seen in every sample
551.13	445.96	Zn-O stretching vibration
441.28 445.79	431.73	Zn-O stretching

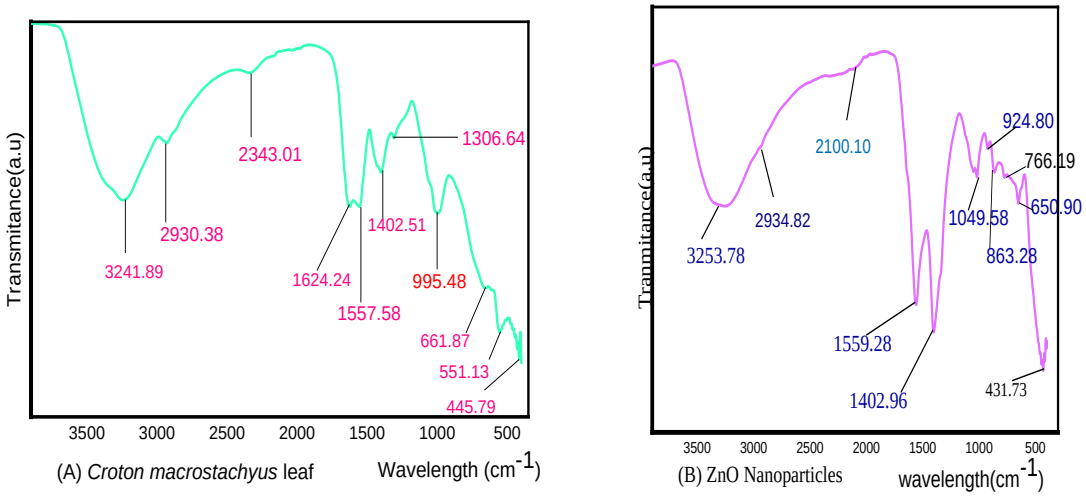

Figure 4. *FTIR Spectra of (A) Croton macrostachyus* leaf extract and (B) ZnO nanoparticles

PXRD diffraction analysis

The PXRD analysis result for ZnO NPs shown in Figure 5, there were peaks at diffraction angles of 2θ (corresponding planes) (31.920 (100), 34.580 (002), 36.420 (101), 47,720 (012), 56.780 (110), 63.150 (103) and 68.160 (112). All of which, in keeping with the standard card (JCPDS No. 36-3411), depict zinc oxide nanoparticles having a hexagonal wurtzite structure. Applying the Debye Scherrer formula to the strongest peaks, seven peaks was computed using origin software.

$$\text{Grain size (D)} = \frac{k\lambda}{\beta cos\,(\theta)} \quad (3)$$

Where λ = 0.15406 nm is the wavelength of the incident Cu Kα radiation, β is the full width at half maximum (FWHM) of the corresponding peak (in degrees), θ is the Braggs angle (in degrees), and k is the Scherer constant (k = 0.90), the grain size of the sample was calculated and tabulated in Table 4, It demonstrates that the size of the nanocomposites was between 15 to 22 nm. Thus, for pure zinc oxide nanoparticles, the two theta was at highest peak from 2θ = 36.420 degree at miller indices (101) for ZnO NPs, consequently the lattice characteristics, such as the lattice parameters of the unit cell a, b, and c of ZnO nanoparticles were calculated and evaluated using Bragg's equations (Jenkin et al., 2001& Jones et al., 2008)

$$\lambda = 2d\sin\theta \quad (4)$$

$$sin\theta = \frac{\lambda}{2a\sqrt{h^2+k^2+l^2}} \quad (5)$$

$$a = \frac{\lambda}{\sqrt{3}\,sin\theta(hkl)} \quad (6)$$

$$c = \frac{\lambda}{sin\theta} \quad (7)$$

Equations (5) to (7) were utilized to compute the parameters of the unit cell, a and c, which are listed in Table 4. Additionally, when the diffraction angle grew, both the size and the d-spacing dropped.

Table 4

XRD peak position, miller indices, and unit cell parameters for ZnO NPs,

Samples	Miller indices (hkl)	2θ (°)	d-spacing	a=b	c	Size (nm)	FWHM (degree)	Average Size (D) (nm)
ZnO NPs	100	31.920	2.7990	3.572	6.180	18.76	0.480	
	002	34.580	2.5920	2.952	5.107	18.86	0.280	
	101	36.420	2.4690	2.872	4.901	18.98	0.440	
	012	47.720	1.8885	2.199	3.804	20.68	0.360	21.03
	110	56.780	1.6175	2.065	3.573	21.00	0.840	
	103	63.150	1.4710	1.809	3.134	21.65	0.480	
	112	68.160	1.3777	1.781	3.081	22.00	0.600	

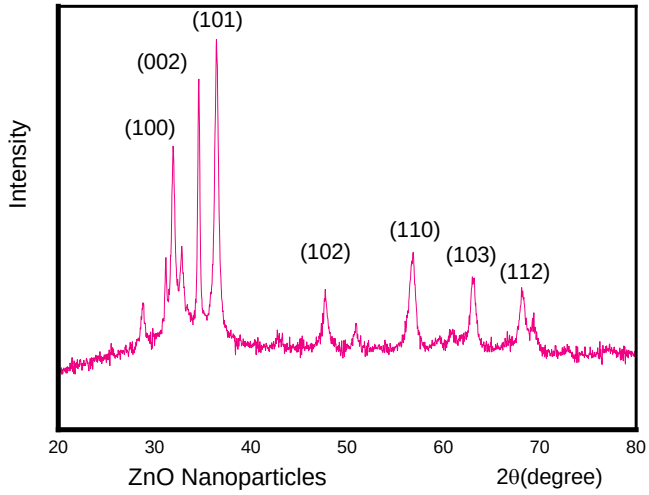

Figure 5. *PXRD spectrum of ZnO Nanoparticles*

X-ray photoelectron spectroscopy (XPS) analysis

To get further insight into the structure's bonding properties, oxidation states, and purity, XPS measurements were reviewed. With different binding energies for ZnO NPs as separate metals in both samples, XPS analysis thus verified the existence of Zn in ZnO NPS. The XPS results of the synthesized ZnO nanoparticles' chemical compositions, valence states, and binding characteristics are displayed in Figure 6(A). The C1s peak, identified at 284.58 eV, may have resulted from carbon dioxide contamination of the samples or from hydrocarbons found in plant extracts. Figure 6 (A) and the binding energies of 292.69 and 288.32 e V, consequently, for the C=O and bonds C-C, respectively. It was evident from the XPS spectrum analysis that the product was ZnO. In the XPS data shown

in Figure 6 (D), the elements zinc, oxygen, distinct peaks were detected for each sample, at 1021.33 eV(2p1/2) and 1044.42 eV($2p_{2/3}$) indicating the high binding energy of the element zinc, Zn $2p^3$. ZnO's lattice oxygen of the produced samples' binding energies, which and carbon were detected. In Figure 6(C), two were approximately 530.36 eV (Figure 6 B)may be attributed to ZnO's lattice oxygen. However, the ZnO sample showed low strength signals from the carbon (C) atom.

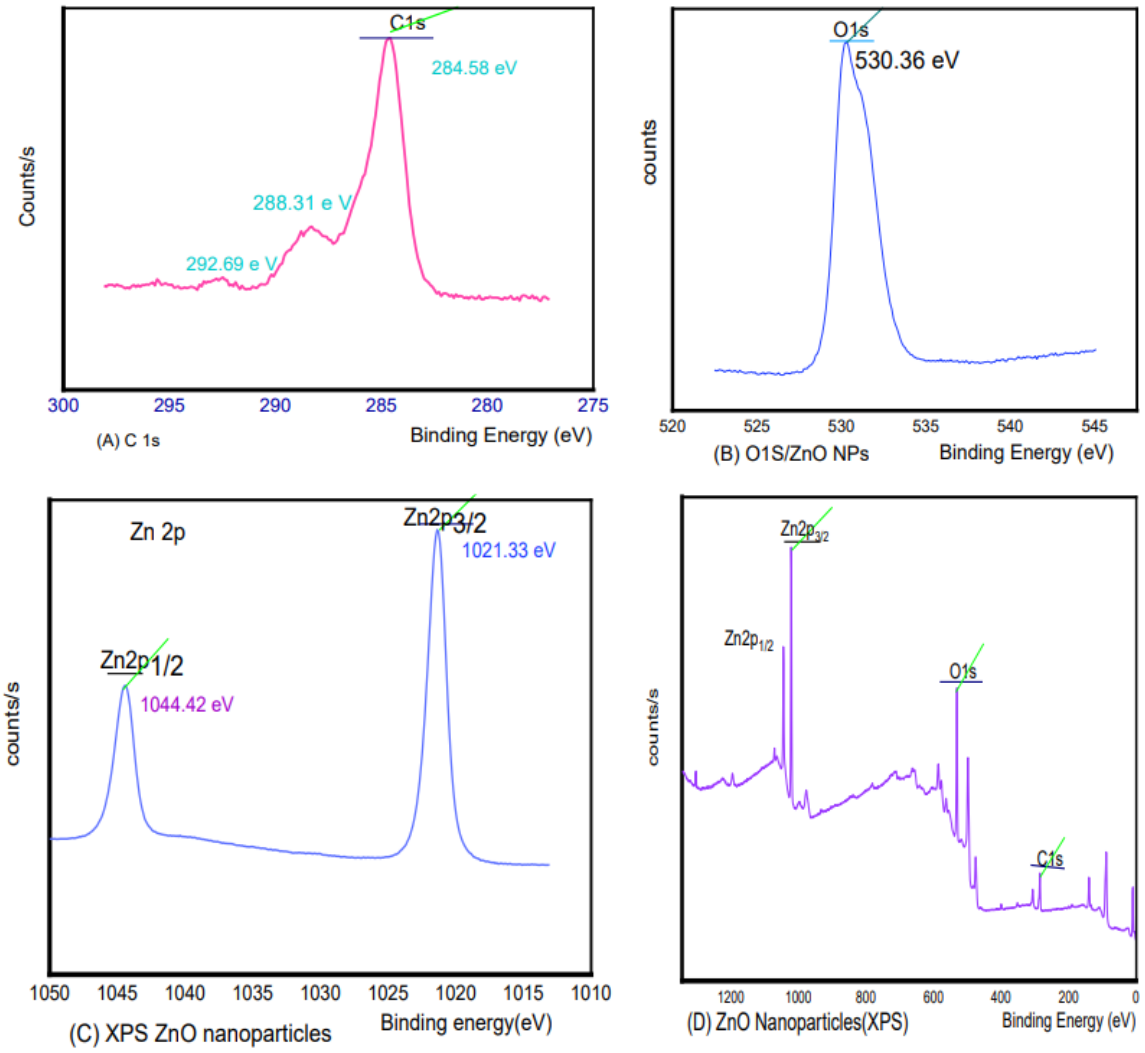

Figure 6. *XPS spectra of ZnO nanoparticles: (A) C 1s,(B) O 1s, (C) Zn 2P and (D) full Survey of ZnO NPs*

Scanning Electron Microscope (SEM) with Energy Dispersive X-ray (EDX) Study SEM is elucidates the sample surface through the use of a high-energy electron beam to scan the samples. X-rays in the SEM can be used to classify then elemental composition of a sample by a method known as EDX the crystal morphologies of the ZnO nanoparticles

were assessed through SEM figure 7 (a,b & c) and EDX displayed as pure ZnO nanoparticles. The shape was flower and rode like the of ZnO nanoparticles synthesized via pyhto-mediated *Croton macrostachyus* Leaf plant was in the nano size range, which was comparable to the data from XRD and TEM.

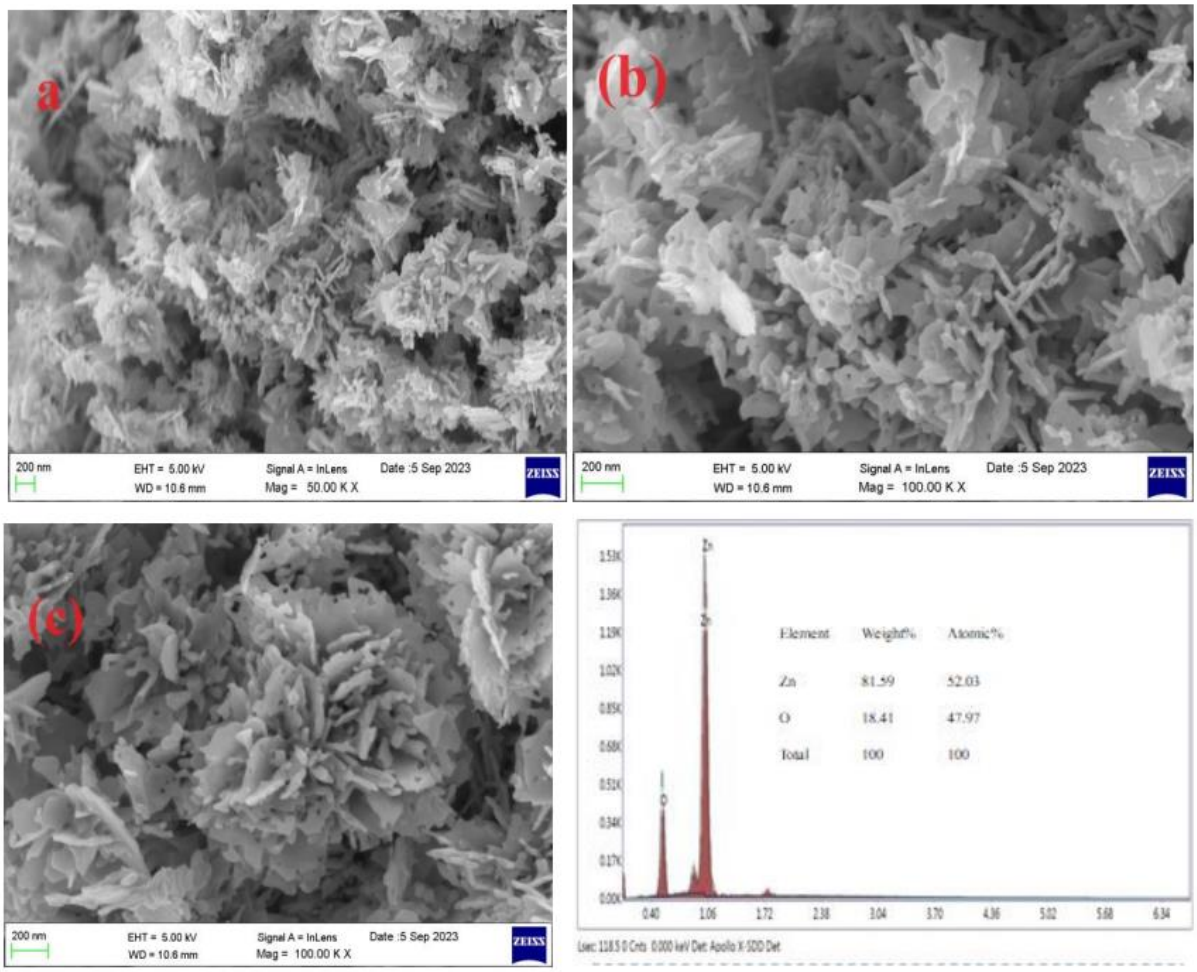

Figure 7. *Images from scanning electron microscopy (SEM) with magnification (a, b & c), and EDX graph*

Selective Area Electron the diffraction Investigation and a High-Resolution Transmission Electron Microscope

Transmission electron microscopy (TEM) shows the morphology and crystal structure of nanoparticles and nano composites. According to the TEM micrograph, ZnO nanoparticles have been determined to be between 10 and 100 nm in size. The morphology of zinc oxide nanoparticles was displayed in the figure 8(a, b, c) with spherical shape and at miller indexes of (101), the lattice plane distance was 0.254 nm.

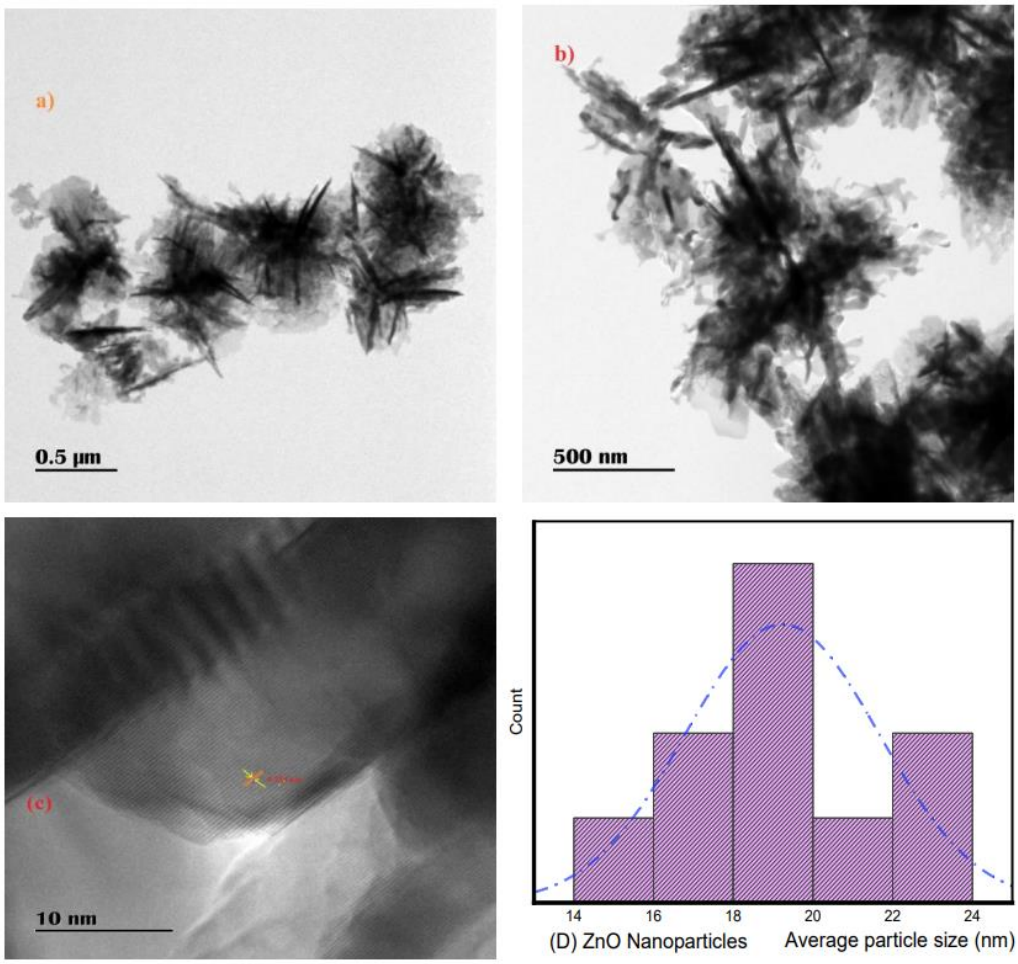

Figure 8. *Images of TEM (a & b), HRTEM pattern (c) and Average particles size distribution (D) of ZnO nanoparticles*

Activities involving antioxidants

Using the DPPH technique, the scavenging capabilities of various ZnO nanoparticle forms were assessed. The stable DPPH's scavenging assessment is often utilized to investigate a material's capacity to scavenge radicals. The decreased DPPH formed by the donation of a proton to antioxidants allowed them to scavenge DPPH radical. ZnO-NPs are able to hold onto DPPH-free radicals with odd electrons through n to π motion because of the transference of electron thickness from oxygen particles to nitrogen molecules (Carofiglio *et al*., 2020). As indicated in figure 9, the scavenging activities of synthesized ZnO NPs were slightly greater than those of normal zinc oxide and the positive control used was ascorbic acid he catalyst driving an increase in activity related to scavenging was zinc oxide nanoparticles. At the maximum dose of 100µg/ml, the radical hunters of ZnO NPs with different mass and ascorbic acid were between 47 to 68 % for lower concentration of 79 to 97% for higher concentration indicates that increased the

scavenging activities were enhanced. In comparison to conventional ascorbic acid, there was a 3.97% increase in the scavenging free radical and ˙OH (Barani *et al*., 2021), as it was observed the different concentration of ZnO nanoparticles displayed in Figure 9, the scavenging activities.

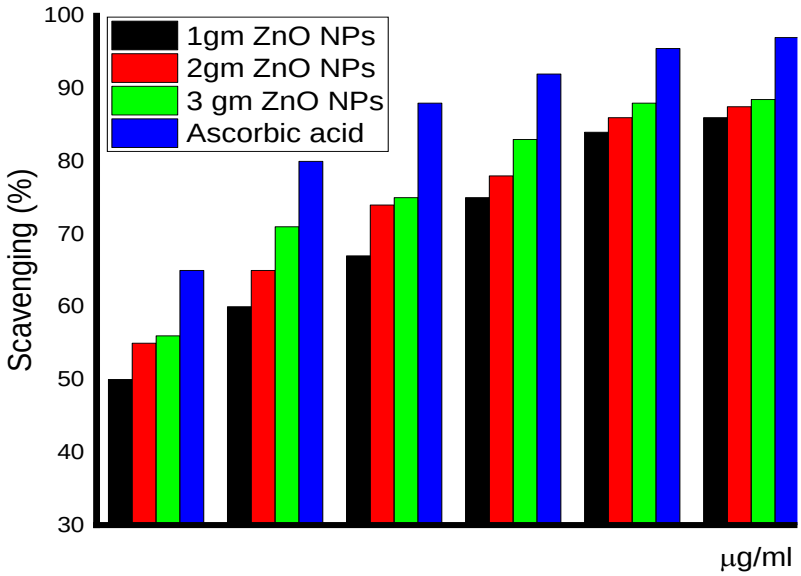

Figure 9. *Anti-oxidant activities of Phyto-mediated synthesized ZnO NPs (1, 2, & 3 gram) and ascorbic acid, with DDPH scavenging (%)*

CONCLUSIONS

ZnO nanoparticles were synthesized in an easy, inexpensive, and environmentally friendly manner by solution combustion method using Croton *macrostachyus* aqueous leaf extract in phyto-mediated synthesis. There is no energy since the secondary metabolites of the extract were utilized in the synthesis as a process-associated reducing, restoring, and capping agent. In this synthesis, $Zn(CH_3COO)_2.3H_2O$ precursors as the source of zinc oxide nanoparticles and different characterization mechanisms were used to confirm the sample was ZnO nanoparticles with nano sized in structure. UV-visible spectroscopy was used to characterize the wave length in nm at highest absorption of ZnO nanoparticles. The stretching and vibration of Zn-O are confirmed by FTIR . The PXRD used to measure the size of zinc oxide nanoparticles which was less than 20 nm. Using SEM, TEM and HRTEM the morphology of the samples was flower like and rode like and conclude that the average crystalline size distribution was between 19 nm to 21 nm also the oxidation state of the samples was confirmed by using XPS. The elemental composition of Zn and O in the ZnO NPs confirmed by the XPS and EDX studies. The Anti-oxidant activities of ZnO nanoparticles was determined by DPPH and ˙OH radical Scavenging and showed better activities

ACKNOWLEDGMENTS

The authors express gratitude to the Department of Chemistry at Wollega University for their support in conducting the

Antioxidant activity. Additionally, the authors would like to acknowledge Adama Science and Technology University in Ethiopia for their contribution to the PXRD and FTIR characterization.

CONFLICTS OF INTEREST

The authors declare that there are no conflicts of interest regarding the publication of this paper.

DATA AVAILABILITY STATEMENTS

The data of this study are available from the corresponding author upon request.

REFERENCES

Ahmad, W., & Kalra, D. (2020). Green synthesis, characterization and anti-microbial activities of ZnO nanoparticles using *Euphorbia hirta* leaf extract. Journal of King Saud University-Science, 32(4), 2358-2364.

Ahmed, S., Chaudhry S.A, Ikram S., (2017) A review on biogenic synthesis of ZnO nanoparticles using plant extracts and microbes: a prospect towards green chemistry. *J. Photochem. Photobiol. B* 166, 272–284

Barani, M., Masoudi, M., Mashreghi, M., Makhdoumi, A., & Eshghi, H. (2021). Cell-free extract assisted synthesis of ZnO nanoparticles using aquatic bacterial strains: Biological activities and toxicological evaluation. *International Journal of Pharmaceutics*, *606*, 120878.

Cahino, A. M., Loureiro, R. G., Dantas, J., Madeira, V. S., & Fernandes, P. C. R. (2019). Characterization and evaluation of ZnO/CuO catalyst in the degradation of methylene blue using solar radiation. *Ceramics International*, *45*(11), 13628-13636.

Carofiglio, M., Barui, S., Cauda, V., & Laurenti, M. (2020). Doped zinc oxide nanoparticles: synthesis, characterization and potential use in nanomedicine. *Applied Sciences*, *10*(15), 5194.

Chen, C., Liu, X., Fang, Q., Chen, X., Liu, T., & Zhang, M. (2020). Self-assembly synthesis of CuO/ZnO hollow microspheres and their photocatalytic performance under natural sunlight. *Vacuum*, *174*, 109198.

Chong, H. W., Rezaei, K., Chew, B. L., & Lim, V. (2018). Chemometric profiling of Clinacanthus nutans leaves possessing antioxidant activities using ultraviolet-visible spectrophotometry. *Chiang Mai J. Sci*, *45*, 1-12.

Danish, M. S. S., Bhattacharya, A., Stepanova, D., Mikhaylov, A., Grilli, M. L., Khosravy, M., & Senjyu, T. (2020). A systematic review of metal oxide applications for energy and environmental sustainability. *Metals*, *10*(12), 1604.

Elemike, E. E., Onwudiwe, D. C., & Singh, M. (2020). Eco-friendly synthesis of copper oxide, zinc oxide and copper oxide–zinc oxide nanocomposites, and their anticancer applications. *Journal of Inorganic and Organometallic Polymers and Materials*, *30*, 400-409.

Faye, G., Jebessa, T., & Wubalem, T. (2022). Biosynthesis, characterization and antimicrobial activity of zinc oxide and nickel doped zinc oxide nanoparticles using Euphorbia abyssinica bark extract. *IET nanobiotechnology*, *16*(1), 25-32.

Gul, R., Jan, S. U., Faridullah, S., Sherani, S., & Jahan, N. (2017). Preliminary phytochemical screening, quantitative analysis of alkaloids, and antioxidant activity of crude plant extracts from Ephedra intermedia indigenous to Balochistan. *The Scientific World Journal*, *2017*.

Jenkin, J. (2001). A unique partnership: William and Lawrence Bragg and the 1915 Nobel Prize in physics. *Minerva*, *39*(4), 373-392.

Jones, N., Ray, B., Ranjit, K. T., & Manna, A. C. (2008). Antibacterial activity of ZnO nanoparticle suspensions on a broad spectrum of microorganisms. *FEMS microbiology letters*, *279*(1), 71-76.

Mansoori, A., Singh, N., Dubey, S. K., Thakur, T. K., Alkan, N., Das, S. N., & Kumar, A. (2020). Phytochemical characterization and assessment of crude extracts from Lantana camara L. for antioxidant and antimicrobial activity. *Frontiers in Agronomy*, *2*, 582268.

Maroyi, A. (2017). Ethnopharmacological uses, phytochemistry, and pharmacological properties of Croton macrostachyus Hochst. Ex Delile: a comprehensive review. *Evidence-Based Complementary and Alternative Medicine*, *2017*.

Masho, T. J., Arasu, P. T., Bogale, R. F., AmareZerrefa, E., & Ramamurthy, S. (2024). Green synthesis, characterization of Ag2O/CuO/ZnO nano composites using aqueous extract of Croton macrostachyus leaf for Photo degradation, anti-microbial and antioxidant activities. *Results in Chemistry*, 101369.

Mutukwa, D., Taziwa, R. T., & Khotseng, L. (2022). Antibacterial and Photodegradation of Organic Dyes Using Lamiaceae-Mediated ZnO Nanoparticles: A Review. *Nanomaterials*, *12*(24), 4469.

Najoom, S., Fozia, F., Ahmad, I., Wahab, A., Ahmad, N., Ullah, R.,& Khan, A. A. (2021). Effective antiplasmodial and cytotoxic activities of synthesized zinc oxide nanoparticles using Rhazya stricta leaf extract. *Evidence-based Complementary and Alternative Medicine*, *2021*, 1-9.

Parbuntari, H., Prestica, Y., Gunawan, R., Nurman, M. N., & Adella, F. (2018). Preliminary phytochemical screening (qualitative analysis) of cacao leaves (Theobroma cacao L.). *EKSAKTA: Berkala Ilmiah Bidang MIPA*, *19*(2), 40-45.

Peralta-Videa, J. R., Huang, Y., Parsons, J. G., Zhao, L., Lopez-Moreno, L., Hernandez-Viezcas, J. A., & Gardea-Torresdey, J. L. (2016). Plant-based green synthesis of metallic nanoparticles: scientific curiosity or a realistic alternative to chemical synthesis. *Nanotechnology for Environmental Engineering*, *1*, 1-29.

Qin, C., Wang, Y., Gong, Y., Zhang, Z., & Cao, J. (2019). CuO-ZnO hetero-junctions decorated graphitic carbon nitride hybrid nanocomposite: hydrothermal synthesis and ethanol gas sensing application. *Journal of Alloys and Compounds*, *770*, 972-980.

Ram, S., & Sinha, V. S. (2015). Qualitative phytochemical analysis of some plants uses to cure malaria in Kolhan region of Jharkhand, India. *J Med Plants Stud*, *3*, 60-62.

Saptarini, N. M., Herawati, I. E., & Permatasari, U. Y. (2016). Total flavonoids content in acidified extract of flowers and leaves of gardenia (Gardenia jasminoides Ellis). *Asian Journal of Pharmaceutical and Clinical Research*, *9*(1), 213-215.

Singh, V., & Kumar, R. (2017). Study of phytochemical analysis and antioxidant activity of Allium sativum of Bundelkhand region. *International Journal of Life-Sciences Scientific Research, 3*(6), 1451-1458.

Tanna, J. A., Chaudhary, R. G., Gandhare, N. V., Rai, A. R., Yerpude, S., & Juneja, H. D. (2016). Copper nanoparticles catalysed an efficient one-pot multicomponents synthesis of chromenes derivatives and its antibacterial activity. *Journal of Experimental Nanoscience*, *11*(11), 884-900.

Terefe, E. M., Okalebo, F. A., Derese, S., Langat, M. K., Mas-Claret, E., Aljarba, N. H., & Muriuki, J. (2022). In vitro anti-HIV and cytotoxic effects of pure compounds isolated from Croton macrostachyus Hochst. Ex Delile. *BMC Complementary Medicine and Therapies*, *22*(1), 159.